



UNIVERSITY OF LEEDS

This is a repository copy of *Extruded low density polyethylene-curcumin film: A hydrophobic ammonia sensor for intelligent food packaging*.

White Rose Research Online URL for this paper:

<https://eprints.whiterose.ac.uk/180563/>

Version: Accepted Version

---

**Article:**

Zhai, X, Wang, X, Zhang, J et al. (9 more authors) (2020) Extruded low density polyethylene-curcumin film: A hydrophobic ammonia sensor for intelligent food packaging. *Food Packaging and Shelf Life*, 26. 100595. ISSN 2214-2894

<https://doi.org/10.1016/j.fpsl.2020.100595>

---

© 2020 Elsevier Ltd. All rights reserved. This manuscript version is made available under the CC-BY-NC-ND 4.0 license <http://creativecommons.org/licenses/by-nc-nd/4.0/>.

**Reuse**

This article is distributed under the terms of the Creative Commons Attribution-NonCommercial-NoDerivs (CC BY-NC-ND) licence. This licence only allows you to download this work and share it with others as long as you credit the authors, but you can't change the article in any way or use it commercially. More information and the full terms of the licence here: <https://creativecommons.org/licenses/>

**Takedown**

If you consider content in White Rose Research Online to be in breach of UK law, please notify us by emailing [eprints@whiterose.ac.uk](mailto:eprints@whiterose.ac.uk) including the URL of the record and the reason for the withdrawal request.



[eprints@whiterose.ac.uk](mailto:eprints@whiterose.ac.uk)  
<https://eprints.whiterose.ac.uk/>

1       **Extruded low density polyethylene-curcumin film: a hydrophobic ammonia**  
2   **sensor for intelligent food packaging**

3       Xiaodong Zhai<sup>a</sup>, Xinyu Wang<sup>a</sup>, Junjun Zhang<sup>a</sup>, Zhikun Yang<sup>a</sup>, Yue Sun<sup>a</sup>, Zhihua Li<sup>a</sup>, Xiaowei  
4       Huang<sup>a</sup>, Melvin Holmes<sup>b</sup>, Yunyun Gong<sup>b</sup>, Megan Povey<sup>b</sup>, Jiyong Shi<sup>a,\*</sup>, Xiaobo Zou<sup>a,\*</sup>

5       <sup>a</sup>*Agricultural Product Processing and Storage Lab, School of Food and Biological Engineering,*  
6       *Jiangsu University, Zhenjiang, Jiangsu 212013, China*

7       <sup>b</sup>*School of Food Science and Nutrition, University of Leeds, Leeds LS2 9JT, United Kingdom*

8       \*Corresponding author. Tel.: +86 511 88780174; Fax: +86 511 88780201; Email:  
9       zou\_xiaobo@ujs.edu.cn (Xiaobo Zou), Shi\_jiyong@ujs.edu.cn (Jiyong Shi).

10 **Abstract**

11 A hydrophobic film was developed using low density polyethylene (LDPE) and  
12 curcumin with the melting extrusion method. The hydrophobic nature of the LDPE  
13 endowed the film with good stability to pH buffer solutions, namely without obvious  
14 color change or curcumin leaching, when immersed in pH buffer solutions. The LDPE-  
15 curcumin composite film was sensitive to ammonia (NH<sub>3</sub>), and the limit of detection  
16 (LOD) of LDPE-curcumin film to NH<sub>3</sub> at 90% RH was 0.18 μM. When the LDPE-  
17 curcumin film was used to monitor beef and silver carp spoilage at 4 °C, it showed light  
18 yellow-to-light brown color changes along with the storage time, resulting from the  
19 increasing TVB-N contents of the meat samples. As the developed LDPE-curcumin  
20 film was totally non-toxic and suitable for industrial production in a large scale, there  
21 will be a good potential for its application in intelligent food packaging.

22 **Keywords**

23 Hydrophobic film; low density polyethylene; curcumin; meat spoilage; intelligent  
24 packaging

## 25 **1. Introduction**

26 Intelligent food packaging has received great attention in modern food industry. It  
27 particularly aims to *in-situ* and real-time monitor the food quality in individual  
28 packages for food quality assessment and safety assurance. To date, various  
29 colorimetric sensors (Lin, et al., 2016; Long, et al., 2019; Zhai, et al., 2019) and  
30 indicators (Saliu & Della Pergola, 2018; Wang, Lu, & Gunasekaran, 2017; C. Zhang,  
31 et al., 2013), and wireless electronic sensors (Koskela, et al., 2015; Z. Ma, et al., 2018;  
32 Zhu, Desroches, Yoon, & Swager, 2017) have been developed for intelligent packaging,  
33 with advantages of good portability, low cost, and easy fabrication. Among them,  
34 colorimetric sensors have been widely studied, because their color changes can be  
35 directly assessed by naked eye or using digital imaging technology.

36 Meat spoilage during distribution can easily occur, due to enzymatic reaction and  
37 microbial contamination. Total volatile basic amines (TVB-N), such as trimethylamines,  
38 dimethylamines and ammonia, are widely regarded as a meat spoilage indicator. To  
39 achieve the real-time evaluation of meat spoilage, a number of studies have tried to use  
40 synthetic pH-sensitive dyes to develop the TVB-N sensors in intelligent packaging  
41 systems (Chun, Kim, & Shin, 2014; Domínguez-Aragón, Olmedo-Martínez, &  
42 Zaragoza-Contreras, 2018; Mo, et al., 2017; A. Pacquit, et al., 2006). Traditionally,  
43 considering of the potential toxicity of the synthetic dyes, pH-sensitive dyes are  
44 generally encapsulated into a polymer and then covered by a gas-permeable and ion-  
45 impermeable membrane (GPM) to prevent the leaching of synthetic dyes from the films  
46 to the humid food packaging environment (Kuswandi, et al., 2012; K. Lee, Baek, Kim,  
47 & Seo, 2019; Wells, Yusufu, & Mills, 2019). Of late, chemical covalent cross-linking  
48 (Jia, et al., 2019) and melting extrusion methods (Wells, et al., 2019) have also been  
49 proposed to embed the pH-sensitive dyes into solid films and simultaneously prevent  
50 the leaching of dyes, which provided new approaches to design colorimetric films for  
51 intelligent food packaging.

52 Although the synthetic pH-sensitive dyes showed good performance in developing  
53 meat quality indicators, it is still highly desirable to develop totally safe colorimetric

54 films (S. J. Lee & Rahman, 2014). In recent years, natural edible pigments, such as  
55 anthocyanins (Dudnyk, Janeček, Vaucher-Joset, & Stellacci, 2018; Q. Ma & Wang,  
56 2016; Zhai, et al., 2018; J. Zhang, et al., 2019), alizarin (Ezati, Tajik, & Moradi, 2019),  
57 betalains (Qin, Liu, Zhang, & Liu, 2020) and curcumin (Kuswandi, Jayus, Larasati,  
58 Abdullah, & Heng, 2011; Liu, et al., 2018; Q. Ma, Du, & Wang, 2017), have been used  
59 to develop pH-sensitive films to monitor meat quality. These pigments are generally  
60 embedded in hydrophilic polymer films, such as chitosan (X. Zhang, Lu, & Chen, 2014),  
61 gelatin (Chayavanich, Thiraphibundet, & Imyim, 2019),  $\kappa$ -carrageenan (Liu, et al.,  
62 2019), polyvinyl alcohol (Qin, et al., 2020) and so forth. However, the big concern is  
63 that the package with fresh meat has high relative humidity (RH), so that the hydrophilic  
64 polymer film could inevitably absorb water from the internal package environment,  
65 which induced the leaching of pigments from the film (Liu, et al., 2019; Liu, et al., 2018;  
66 Q. Ma, et al., 2017; Zhai, et al., 2020). Even though the leaching of natural pigments  
67 would not lead to food safety issues, it should have great effect on the indicating  
68 property of the film due to the unpredictable fluctuation of pigment content in the film  
69 caused by leaching (S. Huang, et al., 2019; Q. Ma, et al., 2017; Zhai, et al., 2017).  
70 Furthermore, the sensing ability of the hydrophilic films to volatile gases may be  
71 susceptible to the humidity of the package environment (Zhai, et al., 2020). Hence,  
72 there is an urgent need to reduce the leaching of the natural pigments and the effect of  
73 humidity on the sensing ability of the film.

74 To meet this requirement, in this study, we tried to develop a hydrophobic  
75 colorimetric film by incorporating natural pigment curcumin in LDPE using the melting  
76 extrusion method. On one hand, curcumin is a low molecular-weight phenolic  
77 compound obtainable from the rhizomes of turmeric (*Curcuma longa* Linn.), and has  
78 been widely used as a food coloring agent owing to its intense yellow color (Xiang,  
79 Sun-Waterhouse, Cui, Wang, & Dong, 2018). On the other hand, LDPE is a nontoxic  
80 polymer and LDPE films have been widely used in food packaging due to its good  
81 mechanical and water barrier properties. A recent study has shown the feasibility of  
82 developing LDPE-curcumin films by using the melting extrusion method (Zia, Paul,

83 Heredia-Guerrero, Athanassiou, & Fragouli, 2019). However, to our best knowledge,  
84 the indicating property of the LDPE-curcumin film, as a colorimetric gas sensor, for  
85 intelligent food packaging has not been reported yet. The experimental results showed  
86 that the LDPE-curcumin film could prevent the leaching of curcumin in buffer solutions.  
87 Meanwhile, the film was sensitive to NH<sub>3</sub> and could exhibit visible color changes when  
88 used to monitor meat spoilage. As the LDPE-curcumin film is nontoxic, cost effective  
89 and fabricated by using the melting extrusion method (Fig. S1), a classical polymer  
90 technological process for large scale industrial production, it presented a promising  
91 method to develop natural pigment based colorimetric films for intelligent packaging.

## 92 **2. Materials and methods**

### 93 2.1. Materials and reagents

94 Fresh beef and live silver carp were bought from a local market (Zhenjiang, China).  
95 LDPE powder was purchased from Shanghai Jiexun Plasticizing Co., Ltd. (Shanghai,  
96 China). Curcumin, magnesium chloride, magnesium nitrate, sodium chloride,  
97 potassium sulphate, citric acid, sodium citrate, hydrochloric acid, sodium hydroxide,  
98 methyl red, methylene blue, and boric acid were purchased from Sinopharm Chemical  
99 Reagent Co., Ltd (Shanghai, China). Gaseous NH<sub>3</sub> was purchased from Thorpe  
100 Chemical Co., Ltd (Zhenjiang, China).

### 101 2.2. Preparation of the LDPE-curcumin film

102 The preparation of LDPE-curcumin film was according to a previous literature with  
103 slight modification (Zia, et al., 2019). First, 1 g of curcumin powder and 100 g of LDPE  
104 powder were mixed by mechanical stirring. The curcumin-covered LDPE powder was  
105 then pelletised using a twinscrew extruder (Baopin International Precision Instruments  
106 Co., Ltd.) with screws of 20 mm diameter, and length to diameter ratio of 40. The  
107 operating temperatures were set at 90, 110, 120, 130 and 130 °C for the feeding, heating  
108 zones 1-3 and pelletising die, respectively. The extruder screw speed was 80 rpm  
109 throughout the extrusion process. The obtained LDPE-curcumin pellets were then  
110 extruded into a thin, clear yellow-colored plastic film with operating temperatures of  
111 130 °C, using a single-screw extruder (Baopin International Precision Instruments Co.,

112 Ltd.) with a screw of 20 mm diameter and length to diameter ratio of 28. The thickness  
113 of the obtained film was  $\sim 50 \mu\text{m}$ . The control LDPE film without curcumin was also  
114 prepared following the same procedures.

### 115 2.3. Response to pH buffer solutions

116 The pH buffer solutions in the range of 2-12 were prepared by using 0.2 M disodium  
117 hydrogen phosphate, 0.2 M citric acid and 0.2 M sodium hydroxide solutions with  
118 different proportions. Curcumin powder was added to the prepared pH buffer solutions  
119 with the addition of 20% ethanol as curcumin has an extremely low solubility. Then,  
120 the UV-Vis spectra of curcumin solutions were recorded. The release of curcumin from  
121 the film to buffer solutions was investigated by immersing 4 g of LDPE-curcumin film  
122 in 100 mL of the buffer solution at 25 °C. The film was taken out from the buffer  
123 solution after every 24 h, and the UV-Vis spectra of the solutions were recorded.

### 124 2.4. Response to $\text{NH}_3$ under different RH

125 First, the LDPE-curcumin film ( $30 \times 10 \text{ mm}$ ) was adhered on the inner surface of the  
126 cuvette. The cuvettes were put in desiccators with silica gels, NaBr saturated solution  
127 and  $\text{Na}_2\text{HPO}_4$  saturated solution for 24 h at 25 °C. The actual RH in the desiccators  
128 were determined to be 6% (silica gels), 55% (NaBr saturated solution), and 95%  
129 ( $\text{Na}_2\text{HPO}_4$  saturated solution), by using a commercial hygrometer (AR837, SMART  
130 SENSOR). The cuvettes were sealed with rubber caps before they were taken out from  
131 the desiccators. A certain amount of  $\text{NH}_3$  was injected into the cuvettes by using needle  
132 syringes. Here, the concentration of  $\text{NH}_3$  was determined by trapping  $\text{NH}_3$  with 10 mL  
133 2% aqueous solution of boric acid and 3 droplets of mixed indicator produced from  
134 dissolution of 0.2 g of methyl red and 0.1 g of methylene blue to 100 mL of ethanol.  
135 After that, the boric acid solution was titrated with a 0.01 M hydrochloric acid solution,  
136 and  $\text{NH}_3$  was quantified by the hydrochloric acid used.

137 The reversibility of the film when reacting with  $\text{NH}_3$  was also investigated (Khattab,  
138 Dacrory, Abou-Yousef, & Kamel, 2019). The film was first reacted with  $80 \mu\text{M}$   $\text{NH}_3$   
139 under 90% RH for 30 min, and then was put in air for 1 h at 25 °C. The UV-vis spectra  
140 of the film before reacting with  $\text{NH}_3$ , after reacting with  $\text{NH}_3$ , and after recovering in

141 air were detected. This process was repeated for 5 times.

## 142 2.5. Stability test of the film at different temperatures

143 The film (30 × 10 mm) was adhered on the inner surface of the cuvette. The cuvette  
144 was placed in a constant temperature and humidity incubator with a fluorescent lamp.  
145 The absorbance at 420 nm of the LDPE-curcumin film was recorded by using the UV-  
146 Vis spectrometer.

## 147 2.6. Application of the film in monitoring meat spoilage

148 Live silver carp was pretreated by removing its innards, head, tail and feathers. Then,  
149 it was cleaned by water and diced. A quantity of 500 g of diced fresh beef and silver  
150 carp were put into a polyethylene terephthalate (PET) box with a buttoned lid. The  
151 dimensions of the box is 165 × 115 × 43 mm (L × W × H). The LDPE-curcumin film  
152 was cut to square (20 × 20 mm) and was put in the headspace of the box. The  
153 experimental setup was according a previous studies (Chun, et al., 2014; Alexis Pacquit,  
154 et al., 2007). As the LDPE-curcumin film is transparent, which is not good for *in-situ*  
155 color measurement, it was put on a white cellulose acetate filter paper (25 × 25 mm)  
156 that served as a background. Then, the filter paper was tightly adhered onto the internal  
157 surface of the PET lid by using adhesive tape (see Fig. S4). The above processes were  
158 conducted in a clean bench. Finally, the PET boxes were placed in an incubator at 4 °C  
159 in a refrigerator. The color parameters of the films were detected by using a portable  
160 colorimeter (CM-2300d, Konica Minolta, Inc., Japan). The chromatic parameters of  $\Delta E$   
161 and  $\Delta C^*$  were calculated according to following equations:

$$162 \quad \Delta E = \sqrt{(L_t^* - L_0^*)^2 + (a_t^* - a_0^*)^2 + (b_t^* - b_0^*)^2} \quad (1)$$

$$163 \quad \Delta C^* = \sqrt{(a_t^* - a_0^*)^2 + (b_t^* - b_0^*)^2} \quad (2)$$

164 where  $L_t^*$ ,  $a_t^*$  and  $b_t^*$  were the color parameters of the LDPE-curcumin film after a  
165 certain storage time, and  $L_0^*$ ,  $a_0^*$  and  $b_0^*$  were the initial color parameters of the LDPE-  
166 curcumin film.

167 The total volatile basic nitrogen (TVB-N) content of meat samples was measured  
168 according to a previous literature (Cai, Chen, Wan, & Zhao, 2011), following the



169 Chinese Standard (GB 5009. 228-2016). Briefly, 20 g of meat sample was put in a  
170 beaker with 100 mL of distilled water, and then crushed by using a tissue homogenizer.  
171 The homogenate was filtered with filter papers to obtain the filtrate. Then, 10 mL of  
172 filtrate was transferred to a Kjeldahl distillation unit. The volatile biogenic amines were  
173 distilled, and the distillate was collected with 10 mL of boric acid solution (20 g/L)  
174 containing 5 droplets of mixed indicator that was made by dissolving 0.2 g of methyl  
175 red and 0.1 g methylene blue in 300 mL ethanol. Finally, the distillate was titrated with  
176 0.01 M HCl solution. The TVB-N content was calculated according to the amount of  
177 HCl used during titration, and expressed as mg/100 g.

178 The total viable counts (TVC) of meat samples were measured using the Plate Count  
179 Agar (Mehdizadeh, Tajik, Langroodi, Molaei, & Mahmoudian, 2020). Meat samples  
180 (25 g) were added to 225 mL of phosphate buffer solution (PBS), and then homogenized  
181 by using a homogenizer (IKA, Germany). The homogeneous solution was then serially  
182 diluted at a ratio of ten (V/V) by using the PBS. 1 mL of the diluted solution was spread  
183 on the surface of the plate count agar medium in Petri dishes, which were further  
184 incubated at 35 °C for 2 days. The bacterial counts were expressed as colony-forming  
185 units (CFU) per gram of meat sample and then transformed to base 10 logarithm values,  
186 namely  $\log_{10}(\text{CFU/g})$ .

## 187 2.7. Statistical analysis

188 All the experiments were conducted in triplicate and the data was expressed as means  
189  $\pm$  standard deviation.

## 190 3. Result and discussion

### 191 3.1. Stability of curcumin during extrusion process

192 In this work, curcumin was embedded into LDPE through extruding method, during  
193 which LDPE powder was heated ( $\leq 130$  °C) to molten state and to mix with curcumin.  
194 Therefore, the stability of curcumin under heating should be investigated. The curcumin  
195 powder was first heated in oven in air, and then exposed to  $\text{NH}_3$ . As shown in Fig. 1,  
196 the curcumin powder did not show obvious color changes after 1 h heating at 130 °C,  
197 but exhibited yellow-to-brown color changes when subsequently reacted with  $\text{NH}_3$ .

198 This result indicated that the curcumin powder maintained its sensitivity to NH<sub>3</sub> after  
199 being heated under 130 °C for 1 h in air. However, it presented yellow-to-dark brown  
200 color change when heated at 180 °C for 1 h, while did not show obvious color changes  
201 exposing to NH<sub>3</sub>. This can be due to that the curcumin powder was intensely oxidized  
202 and decomposed to ferulic acid and 4-vinyl guaiacol under 180 °C (Esatbeyoglu,  
203 Ulbrich, Rehberg, Rohn, & Rimbach, 2015), and therefore lost the reactivity with NH<sub>3</sub>.  
204 Hence, the melting temperature ( $\leq 130$  °C) during the extruding process would not  
205 significantly induce the oxidative decomposition of curcumin. In addition, the  
206 pelletizing process was conducted in vacuum condition, which can prevent curcumin  
207 from being oxidized. As shown in Fig. 1, the LDPE-curcumin film presented a light  
208 yellow color, and turned to light brown in response to NH<sub>3</sub>, indicating its sensing ability  
209 to NH<sub>3</sub>. Furthermore, the incorporation of curcumin had no significant effect on the  
210 microstructure of LDPE film. As shown in Fig. S2, the LDPE-curcumin film had a  
211 dense cross section similar to that of the LDPE film. No big particle agglomerates, air  
212 gaps, cracks, or detachment zones were evident, which was in line with a previous study  
213 (Zia, et al., 2019). These results indicated that curcumin, as a natural pigment, can be  
214 embedded into LDPE through extruding technology, and the fabricated LDPE-  
215 curcumin film was sensitive to NH<sub>3</sub>.

### 216 3.2. Response of curcumin and LDPE-curcumin film to pH buffer solutions

217 As mentioned, the package with fresh meat generally has high RH, and the volatile  
218 water vapor would be adsorbed on the surface of the film fixed on the headspace of the  
219 packages. As a result, some non-neutral gases, such as volatile amines (primary and  
220 secondary amines), carbon dioxide and hydrogen sulfide, generated from meats would  
221 partially dissolve and then hydrolyze or ionize in the adsorbent water before they  
222 directly diffused into the films. This would therefore make the film exposed to a non-  
223 neutral aqueous microenvironment. Therefore, the stability of the LDPE-curcumin film  
224 in pH buffer solutions which simulated the non-neutral aqueous microenvironment was  
225 investigated.

226 Firstly, the colors and UV-Vis spectra of curcumin solutions were investigated, as

227 shown in Fig. 2. Curcumin solution showed nearly the same yellow color at pH 2-8,  
228 while turned to brown at pH 9-10 and then reddish brown at pH 11-12 (Fig. 2A), which  
229 was line with a previous study (Pourreza & Golmohammadi, 2015). Correspondingly,  
230 the UV-Vis spectra of curcumin solution showed a maximum absorption peak at nearly  
231 420 nm at pH 2-8, and the absorbance values slightly decreased with the increase of pH  
232 (Fig. 2B). When pH increased from 9 to 12, the maximum absorption peak gradually  
233 shifted to 474 nm, and simultaneously the absorbance values rose. The color and  
234 spectral changes of curcumin solutions with the increase of pH was due to the  
235 deprotonation of curcumin molecular, as described in previous studies (Kotha & Luthria,  
236 2019; Liu, et al., 2018; Priyadarsini, 2014).

237 However, the LDPE-curcumin film did not show color changes even being immersed  
238 in pH buffer solutions for 6 h (Fig. 2C). This insensitivity of LDPE-curcumin film to  
239 pH buffer solutions was further confirmed by the UV-Vis spectra. As shown in Fig. 2D,  
240 the LDPE-curcumin films showed nearly the same spectra at pH 2-12, and the range  
241 value of the maximum absorbance at 420 nm ( $A_{420}$ ) was lower than 0.01 (Fig. 2D inset).  
242 The  $L^*$ ,  $a^*$  and  $b^*$  values of the film were shown in Table S2, indicating no significant  
243 difference between the colors of the films. These results could be due to that curcumin  
244 was embedded in LDPE molecular to reduce the contact between curcumin and water  
245 molecular. Similar phenomenon was also found in an extruded LDPE-bromophenol  
246 blue film (Wells, et al., 2019). Apart from this, the presence of curcumin could also  
247 reduce the water permeability of LDPE film (Zia, et al., 2019), which could also reduce  
248 the contact between curcumin and water.

249 To further investigate the stability of the LDPE-curcumin film in pH buffer solutions,  
250 the LDPE-curcumin film was immersed into buffer solutions for 5 d, and the UV-Vis  
251 spectra of the lixiviums were determined every day. Fig. 2E shows the photo of  
252 lixiviums of the LDPE-curcumin films at the 5<sup>th</sup> d. The lixiviums were nearly colorless  
253 and transparent at pH 2-10, but showed weak yellow at pH 11-12. The corresponding  
254  $A_{420}$  values of the lixiviums were shown in Fig. 2F. All the lixiviums showed low  $A_{420}$   
255 values that were below 0.03 with weak fluctuations within 5 d, indicating the low

256 curcumin contents in the lixiviums. The slightly higher  $A_{420}$  values at pH 11 and 12  
257 might be due to the better solubility of curcumin at basic condition (Priyadarsini, 2014).  
258 In addition, the color of the LDPE-curcumin film remained yellow at the 5<sup>th</sup> d, even at  
259 pH 11 and 12 (Fig. 2F inset). These results indicated that the leaching of curcumin from  
260 the LDPE-curcumin to the pH solution was extremely low.

### 261 3.3. Response of LDPE-curcumin film to NH<sub>3</sub> under different relative humidity

262 The response of LDPE-curcumin film to NH<sub>3</sub> under different relative humidity (RH)  
263 was shown in Fig. 3A. The films turned from light yellow to brown after exposed to  
264 NH<sub>3</sub> at 6%, 55% and 95% RH (Fig. 3A inset). The corresponding UV-Vis spectra  
265 showed that the maximum absorption peak shifted from ~ 420 nm to ~ 460 nm. It can  
266 be also seen that a relative lower RH is good for the reaction between LDPE-curcumin  
267 film and NH<sub>3</sub>, as LDPE-curcumin showed a deeper brown color and higher absorbance  
268 value at ~ 460 nm after exposed to NH<sub>3</sub> under 6% RH than 55% RH, and followed by  
269 95% RH.

270 As mentioned above, the LDPE-curcumin film was insensitive to pH buffer solutions,  
271 but sensitive to NH<sub>3</sub>. These results indicated that the reaction between curcumin and  
272 NH<sub>3</sub> is a solid-gas interaction. Although this does not exclude the possibility of there  
273 being some water present, the water content is likely to be very small (Mills, Wild, &  
274 Chang, 1995). The proposed reaction mechanism was shown in Fig. 3B. The diketo  
275 group of curcumin could exhibit keto-enol tautomerism, and the enal form contains  
276 three labile protons (Priyadarsini, 2014). When NH<sub>3</sub> diffused into the LDPE-curcumin  
277 film (Karim, Hijaz, Kastner, & Smith, 2011; Wells, et al., 2019), it could make the  
278 deprotonation of these three active groups of curcumin, and thus inducing the color and  
279 the spectral changes. This reaction could be described as Equations 3 and 4 (Mills, et  
280 al., 1995). Hence, the reason that a lower RH contributed to the reaction between  
281 LDPE-curcumin film and NH<sub>3</sub> may be that more NH<sub>3</sub> molecular had dissolved into  
282 water under a higher RH to form NH<sub>3</sub>·H<sub>2</sub>O, and then was ionized into NH<sub>4</sub><sup>+</sup> and OH<sup>-</sup>,  
283 while the OH<sup>-</sup> in water drop could not easily diffuse into the film and make the color  
284 changes of curcumin.



287 where  $\text{NH}_3(\text{g})$  is the gaseous ammonia,  $K_H$  is Henry's constant for gaseous ammonia in  
288 the plastic film.  $\text{NH}_3(\text{dis})$  is the gaseous ammonia dissolved in the plastic film. HR is  
289 the protonated form of curcumin.  $K_1$  is an ion-pair formation constant (which depends  
290 strongly upon the dissociation equilibrium constant,  $K_a$ , of curcumin) and  $\text{NH}_4^+\text{R}^-$  is  
291 the ion-pair formed between the dissolved ammonia and HR.

292 The effect of humidity on the hydrophobicity LDPE-curcumin film was quite  
293 different from the hydrophilic films incorporated with curcumin that were reported in  
294 recent studies (Liu, et al., 2018; Q. Ma, et al., 2017), where it was proposed that  $\text{NH}_3$   
295 firstly combined with  $\text{H}_2\text{O}$  in the hydrophilic films or the environment surrounding the  
296 films, and then the ionized  $\text{OH}^-$  induced the color change of curcumin. As a result, the  
297 higher RH was beneficial to the generation of more  $\text{OH}^-$ , accelerating the color change  
298 of the hydrophilic films (Q. Ma, et al., 2017). However, the reaction mechanism  
299 between  $\text{NH}_3$  and curcumin in the presence or absence of water may need to be further  
300 investigated.

#### 301 3.4. Sensitivity of the film to $\text{NH}_3$

302 The sensitivity of the film to  $\text{NH}_3$  was determined at 90% RH, because the packages  
303 containing fresh meats (with water coefficients  $\sim 0.99$ ) generally have high RH. Fig.  
304 4A shows the UV-Vis spectra of the film in response to increasing contents of  $\text{NH}_3$ . The  
305 maximum absorption peak gradually shifted from  $\sim 420$  nm to  $\sim 474$  nm, which was  
306 consistent with the changes of UV-Vis spectra of curcumin solutions with increasing  
307 pH (see section 3.2). The maximum absorbance value at 420 nm showed a continuous  
308 decrease while the absorbance value at 540 nm increased, with the increase of  $\text{NH}_3$   
309 concentration. Generally, visible color absorbs light of wavelengths corresponding to  
310 its complementary color (Choi, Lee, Lacroix, & Han, 2017). Yellow color absorbs light  
311 of wavelength corresponding to its complementary color, blue ( $\sim 400$ - $480$  nm), and red  
312 color absorbs light of the wavelength corresponding to its complementary color, green

313 (~ 495-570 nm). Hence, the absorbance ratio at 540 nm versus 420 nm ( $A_{540}/A_{420}$ ),  
314 wavelength of each complementary color, could indicate the increase of red color  
315 intensity compared to yellow color intensity, with a deeper red color when  $A_{540}/A_{420}$   
316 value was high. As shown in Fig. 4B, the  $A_{540}/A_{420}$  value increased with the  $\text{NH}_3$   
317 concentration, indicating that the color of the film gradually presented a yellow-to-red  
318 transition. In addition, the calibration curves showed that the  $A_{540}/A_{420}$  value had good  
319 linear relationship with the  $\text{NH}_3$  concentration in the range of 0-80  $\mu\text{M}$  and 100-240  
320  $\mu\text{M}$ , with  $R^2$  of 0.9906 and 0.9897, respectively. Accordingly, the limit of detection  
321 (LOD) of the LDPE-curcumin film to  $\text{NH}_3$  was determined to be 0.18  $\mu\text{M}$ , by using  
322 Equation 5 (Courbat, Briand, Damon-Lacoste, Wöllenstein, & de Rooij, 2009):

$$323 \quad LOD = \frac{3K}{N} \quad (5)$$

324 where  $K$  is the standard deviation of blank measurements and  $N$  is slope of the  
325 calibration curve (0.9906).

326 The LOD of LDPE-curcumin film was comparable to that of some other colorimetric  
327 sensors (see Table S2). It is generally expected that the sensing film could have high  
328 sensitivity to  $\text{NH}_3$ . There are several key factors of the pigments (or dyes) based  
329 colorimetric film that determine the sensitivity: (1) The acid dissociation constant ( $\text{p}K_a$ )  
330 value of a pigment. Generally, a lower  $\text{p}K_a$  of the pigment is good for its color change  
331 (Mills, et al., 1995). (2) The content of pigments. A relatively lower content of pigment  
332 in the film was conducive to the sensitivity (Zhai, et al., 2017). (3) The microstructure  
333 of the film. For example, porous structure generally could improve the sensitivity  
334 because it could provide much more contact areas between the pigments and target  
335 gases (Luo & Lim, 2020). However, it should be noted that when more attention have  
336 been paid to improving the sensitivity of the films, their stabilities (e.g. under oxygen  
337 and high RH environment during storage and usage) ought to be considered at the same  
338 time.

339 The response of the film to  $\text{NH}_3$  was reversible, namely the film could recover its  
340 color after it was separated from  $\text{NH}_3$ . As shown in Fig. S3, the initial  $A_{540}/A_{420}$  value

341 of the LDPE-curcumin film was 0.4232, while it increased to 0.7302 after reacting with  
342  $\text{NH}_3$  for the first time. Then, the  $A_{540}/A_{420}$  value decreased to 0.4203 when the film was  
343 separated from  $\text{NH}_3$  and put in air for 1 h. This meant that the film could almost recover  
344 to its original color. This reaction cycle was repeated for 5 times. Finally, when the film  
345 was reacted with  $\text{NH}_3$  and then recovered in air, the  $A_{540}/A_{420}$  values were 0.7172 and  
346 0.4343, respectively, which were close to  $A_{540}/A_{420}$  values of the first reaction cycle.  
347 Hence, the response of the film to  $\text{NH}_3$  was reversible.

### 348 3.5. Stability of the film during storage

349 A good stability for a colorimetric film during storage is important. The  $A_{420}$  values  
350 of the LDPE-curcumin film stored under visible light along with time were shown in  
351 Fig. 5. The  $A_{420}$  value of the film showed gradual decrease with storage at 4, 25 and  
352 37 °C. This instability of the film could be due to the photodecomposition by loss of  
353 two hydrogen atoms from the curcumin molecule, according to a previous study  
354 (Tønnesen, Karlsen, & van Henegouwen, 1986). It was obvious that a lower storage  
355 temperature was conducive to the stability of the film. The  $A_{420}$  values decreased by  
356 4.2%, 7.3% and 15.3% after respectively stored at 4, 25 and 37 °C for 16 d. Hence, the  
357 LDPE-curcumin film was better to be stored or used at a low temperature to reduce its  
358 decomposition.

### 359 3.6. Application of films in monitoring meat spoilage

360 The LDPE-curcumin film was used to monitor silver carp and beef spoilage in a PET  
361 box, as shown in Fig. 6A and 6B, respectively. The color of the LDPE-curcumin film  
362 was shown in Table S3. The initial  $L^*$  of the film was 86.89, which decreased to 68.96  
363 after 1 day storage of silver carp, while  $a^*$  and  $b^*$  did not significantly change. Similar  
364 phenomenon was also observed from the film used for beef. This was because the filter  
365 paper and the LDPE-curcumin film were wetted by water vapor, leading to a decrease  
366 of light of the film. For both the silver carp and beef packaging, the corresponding  $a^*$   
367 value of the LDPE-curcumin film increased, while the  $b^*$  value decreased, indicating a  
368 gradually stronger red color and a weaker yellow color. Hence, the chromatic parameter  
369  $\Delta C^*$ , which depends on the changes of  $a^*$  and  $b^*$ , was used to describe the color changes

370 of the film. It can be seen that the  $\Delta C^*$  values of the film used for silver carp gradually  
371 increased from 0 to 8.25 after storage for 7 days. Meanwhile, the TVB-N value of silver  
372 carp increased from 5.95 to 29.31 mg/100 g. Similarly, the  $\Delta C^*$  values of the film used  
373 for beef gradually increased from 0 to 8.25 after storage for 7 days as well, and the  
374 TVB-N value of beef increased from 6.34 to 26.21 mg/100 g. The increase of TVB-N  
375 with storage time for silver carp and beef was in line with previous studies (Ezati, et al.,  
376 2019; Kachele, Zhang, Gao, & Adhikari, 2017). These results indicated that the LDPE-  
377 curcumin film could present a yellow-to-brown color change resulting from reacting  
378 with the volatile amines of the meats.

379 According to Chinese Standard GB 2707-2016, the rejection limits of TVB-N are 20  
380 and 15 mg/100 g for silver carp and beef, respectively. In this study, the TVB-N value  
381 of silver carp increased to 20 mg/100 g at nearly 5.3 d, when the  $\Delta C^*$  value of the film  
382 was nearly 3.5 (Fig. 6C). This indicated that if the  $\Delta C^*$  value of the film was higher  
383 than 3.5, then the silver carp sample should not be consumed. Similarly, the TVB-N  
384 value of beef sample rose to 15 mg/100 g at nearly 4.2 d, when the  $\Delta C^*$  of the film was  
385 nearly 2.2 (Fig. 6D), indicating that the beef sample should be discarded at this point.

386 TVC is generally used to evaluate the meat spoilage as well (L. Huang, Zhao, Chen,  
387 & Zhang, 2013). The TVC of silver carp and beef during storage at 4 °C was shown in  
388 Table S3. The TVC of silver carp and beef increased respectively from 3.31 to 9.65  
389  $\log_{10}(\text{CFU/g})$ , and from 3.55 to 9.49  $\log_{10}(\text{CFU/g})$ . Similar outcomes have been found  
390 in previous studies (Mehdizadeh, et al., 2020; Zhai, et al., 2019). According to  
391 International Commission on Microbiological Specifications for Food (ICMSF) (Gould,  
392 1990), the maximum acceptable limit for fresh fish is  $10^7$  CFU/g. In this study, the TVC  
393 of silver carp increased to 7  $\log_{10}(\text{CFU/g})$  at nearly 5 d. This indicated that silver carp  
394 could not be consumed after 5-days storage, which was similar to the result of the  
395 TVBN analysis. In addition, according to the European legislation (European  
396 Commission, 2007), the maximum acceptable limit for raw meats is  $5 \times 10^6$  CFU/g. In  
397 this study, the TVC of beef increased to  $\log_{10}(5 \times 10^6 \text{ CFU/g})$ , namely 6.7  $\log_{10}(\text{CFU/g})$ ,  
398 just after 4 d. This indicated that the beef sample could not be consumed after 4 d, which



399 was also similar to the result of the TVBN analysis.

400 It is generally expected that the film could indicate the meat spoilage as early as  
401 possible, and the color changes are highly visible for naked eye for practical application.  
402 In this study, the color differences of the film could be clearly seen after 5 days. Hence,  
403 improving the gas sensitivity of the film to make the film a better indicating property  
404 would be the focus of our further study.

#### 405 **4. Conclusions**

406 LDPE-curcumin film was successfully developed through the melting extrusion  
407 method. The LDPE-curcumin film, as a hydrophobic film, could prevent the leaching  
408 of curcumin under high RH environment. The LDPE-curcumin film was sensitive to  
409 NH<sub>3</sub>, and a lower RH was conducive to the sensitivity. The LOD of LDPE-curcumin  
410 film to NH<sub>3</sub> was determined to be 0.18 μM at 90% RH. The LDPE-curcumin film  
411 showed yellow-to-brown color changes with the storage of silver carp and beef at 4 °C.  
412 As the film is safe, low cost and suitable for industrial production, it would have a good  
413 potential for application in intelligent food packaging.

#### 414 **Declaration of competing interest**

415 None

#### 416 **Acknowledgments**

417 The authors gratefully acknowledge the financial support provided by the National Key  
418 Research and Development Program of China (2017YFC1600806, 2016YFD0401104),  
419 the National Natural Science Foundation of China (31801631, 31671844, 31601543),  
420 the Natural Science Foundation of Jiangsu Province (BK20160506, BE2016306,  
421 BK20180865), International Science and Technology Cooperation Project of Jiangsu  
422 Province (BZ2016013), the Postgraduate Research & Practice Innovation Program of  
423 Jiangsu Province (KYCX17\_1798), and the China Scholarship Council.

424 **References**

- 425 Cai, J., Chen, Q., Wan, X., & Zhao, J. (2011). Determination of total volatile basic nitrogen (TVB-N)  
426 content and Warner-Bratzler shear force (WBSF) in pork using Fourier transform near infrared  
427 (FT-NIR) spectroscopy. *Food Chemistry*, *126*(3), 1354-1360.
- 428 Chayavanich, K., Thiraphibundet, P., & Imyim, A. (2019). Biocompatible film sensors containing red  
429 radish extract for meat spoilage observation. *Spectrochimica Acta Part A: Molecular and*  
430 *Biomolecular Spectroscopy*, *226*, 117601-117606.
- 431 Choi, I., Lee, J. Y., Lacroix, M., & Han, J. (2017). Intelligent pH indicator film composed of agar/potato  
432 starch and anthocyanin extracts from purple sweet potato. *Food Chemistry*, *218*, 122-128.
- 433 Chun, H.-N., Kim, B., & Shin, H.-S. (2014). Evaluation of a freshness indicator for quality of fish  
434 products during storage. *Food Science and Biotechnology*, *23*(5), 1719-1725.
- 435 Commission, E. (2007). Commission Regulation (EC) No 1441/2007 of 5 December 2007 amending  
436 Regulation (EC) No 2073/2005 on microbiological criteria for foodstuffs. *Official Journal of*  
437 *the European Union*, *332*, 12-29.
- 438 Courbat, J., Briand, D., Damon-Lacoste, J., Wöllenstein, J., & de Rooij, N. F. (2009). Evaluation of pH  
439 indicator-based colorimetric films for ammonia detection using optical waveguides. *Sensors*  
440 *and Actuators B: Chemical*, *143*(1), 62-70.
- 441 Domínguez-Aragón, A., Olmedo-Martínez, J. A., & Zaragoza-Contreras, E. A. (2018). Colorimetric  
442 sensor based on a poly(ortho-phenylenediamine-co-aniline) copolymer for the monitoring of  
443 tilapia (*Oreochromis niloticus*) freshness. *Sensors and Actuators B: Chemical*, *259*, 170-176.
- 444 Dudnyk, I., Janeček, E.-R., Vaucher-Joset, J., & Stellacci, F. (2018). Edible sensors for meat and seafood  
445 freshness. *Sensors and Actuators B: Chemical*, *259*, 1108-1112.
- 446 Esatbeyoglu, T., Ulbrich, K., Rehberg, C., Rohn, S., & Rimbach, G. (2015). Thermal stability, antioxidant,  
447 and anti-inflammatory activity of curcumin and its degradation product 4-vinyl guaiacol. *Food*  
448 *& Function*, *6*(3), 887-893.
- 449 Ezati, P., Tajik, H., & Moradi, M. (2019). Fabrication and characterization of alizarin colorimetric  
450 indicator based on cellulose-chitosan to monitor the freshness of minced beef. *Sensors and*  
451 *Actuators B: Chemical*, *285*, 519-528.
- 452 Gould, G. (1990). Micro-organisms in foods 2. Sampling for microbiological analysis: Principles and  
453 specific applications: ICMSF, Blackwell Scientific Publications, London, 1986, 2nd Edn, 293  
454 pp., ISBN 0-632-01567-5.
- 455 Huang, L., Zhao, J., Chen, Q., & Zhang, Y. (2013). Rapid detection of total viable count (TVC) in pork  
456 meat by hyperspectral imaging. *Food Research International*, *54*(1), 821-828.
- 457 Huang, S., Xiong, Y., Zou, Y., Dong, Q., Ding, F., Liu, X., & Li, H. (2019). A novel colorimetric indicator  
458 based on agar incorporated with *Arnebia euchroma* root extracts for monitoring fish freshness.  
459 *Food Hydrocolloids*, *90*, 198-205.
- 460 Jia, R., Tian, W., Bai, H., Zhang, J., Wang, S., & Zhang, J. (2019). Amine-responsive cellulose-based  
461 ratiometric fluorescent materials for real-time and visual detection of shrimp and crab freshness.  
462 *Nature Communications*, *10*(1), 795-802.
- 463 Kachele, R., Zhang, M., Gao, Z., & Adhikari, B. (2017). Effect of vacuum packaging on the shelf-life of  
464 silver carp (*Hypophthalmichthys molitrix*) fillets stored at 4 °C. *Lwt-Food Science and*  
465 *Technology*, *80*, 163-168.
- 466 Karim, F., Hijaz, F., Kastner, C. L., & Smith, J. S. (2011). Ammonia gas permeability of meat packaging

467 materials. *Journal of Food Science*, 76(2), T59-64.

468 Khattab, T. A., Dacrory, S., Abou-Yousef, H., & Kamel, S. (2019). Development of microporous  
469 cellulose-based smart xerogel reversible sensor via freeze drying for naked-eye detection of  
470 ammonia gas. *Carbohydrate Polymers*, 210, 196-203.

471 Koskela, J., Sarfraz, J., Ihalainen, P., Määttänen, A., Pulkkinen, P., Tenhu, H., Nieminen, T., Kilpelä, A.,  
472 & Peltonen, J. (2015). Monitoring the quality of raw poultry by detecting hydrogen sulfide with  
473 printed sensors. *Sensors and Actuators B: Chemical*, 218, 89-96.

474 Kotha, R. R., & Luthria, D. L. (2019). Curcumin: biological, pharmaceutical, nutraceutical, and  
475 analytical aspects. *Molecules*, 24(16).

476 Kuswandi, B., Jayus, Larasati, T. S., Abdullah, A., & Heng, L. Y. (2011). Real-time monitoring of shrimp  
477 spoilage using on-package sticker sensor based on natural dye of curcumin. *Food Analytical  
478 Methods*, 5(4), 881-889.

479 Kuswandi, B., Jayus, Restyana, A., Abdullah, A., Heng, L. Y., & Ahmad, M. (2012). A novel colorimetric  
480 food package label for fish spoilage based on polyaniline film. *Food Control*, 25(1), 184-189.

481 Lee, K., Baek, S., Kim, D., & Seo, J. (2019). A freshness indicator for monitoring chicken-breast spoilage  
482 using a Tyvek® sheet and RGB color analysis. *Food Packaging and Shelf Life*, 19, 40-46.

483 Lee, S. J., & Rahman, A. T. M. M. (2014). Chapter 8 - Intelligent packaging for food products. In J. H.  
484 Han (Ed.), *Innovations in Food Packaging (Second Edition)* (pp. 171-209). San Diego:  
485 Academic Press.

486 Lin, T., Wu, Y., Li, Z., Song, Z., Guo, L., & Fu, F. (2016). Visual monitoring of food spoilage based on  
487 hydrolysis-induced silver metallization of Au nanorods. *Analytical Chemistry*, 88(22), 11022-  
488 11027.

489 Liu, J., Wang, H., Guo, M., Li, L., Chen, M., Jiang, S., Li, X., & Jiang, S. (2019). Extract from *Lycium  
490 ruthenicum Murr.* incorporating  $\kappa$ -carrageenan colorimetric film with a wide pH-sensing range  
491 for food freshness monitoring. *Food Hydrocolloids*, 94, 1-10.

492 Liu, J., Wang, H., Wang, P., Guo, M., Jiang, S., Li, X., & Jiang, S. (2018). Films based on  $\kappa$ -carrageenan  
493 incorporated with curcumin for freshness monitoring. *Food Hydrocolloids*, 83, 134-142.

494 Long, L., Cao, S., Jin, B., Yuan, X., Han, Y., & Wang, K. (2019). Construction of a novel fluorescent  
495 probe for on-site measuring hydrogen sulfide levels in food samples. *Food Analytical Methods*,  
496 12(4), 852-858.

497 Luo, X., & Lim, L.-T. (2020). Curcumin-loaded electrospun nonwoven as a colorimetric indicator for  
498 volatile amines. *Lwt-Food Science and Technology*, 128, 109493-109503.

499 Ma, Q., Du, L., & Wang, L. (2017). Tara gum/polyvinyl alcohol-based colorimetric NH<sub>3</sub> indicator films  
500 incorporating curcumin for intelligent packaging. *Sensors and Actuators B: Chemical*, 244, 759-  
501 766.

502 Ma, Q., & Wang, L. (2016). Preparation of a visual pH-sensing film based on tara gum incorporating  
503 cellulose and extracts from grape skins. *Sensors and Actuators B: Chemical*, 235, 401-407.

504 Ma, Z., Chen, P., Cheng, W., Yan, K., Pan, L., Shi, Y., & Yu, G. (2018). Highly sensitive, printable  
505 nanostructured conductive polymer wireless sensor for food spoilage detection. *Nano Letters*,  
506 18(7), 4570-4575.

507 Mehdizadeh, T., Tajik, H., Langroodi, A. M., Molaei, R., & Mahmoudian, A. (2020). Chitosan-starch  
508 film containing pomegranate peel extract and *Thymus kotschyanus* essential oil can prolong the  
509 shelf life of beef. *Meat Science*, 163, 108073-108083.

510 Mills, A., Wild, L., & Chang, Q. (1995). Plastic colorimetric film sensors for gaseous ammonia.

511 *Microchimica Acta*, 121(1-4), 225-236.

512 Mo, R., Quan, Q., Li, T., Yuan, Q., Su, T., Yan, X., Qian, Z. J., Hong, P., Zhou, C., & Li, C. (2017). An  
513 intelligent label for freshness of fish based on a porous anodic aluminum membrane and  
514 bromocresol green. *ChemistrySelect*, 2(28), 8779-8784.

515 Pacquit, A., Frisby, J., Diamond, D., Lau, K. T., Farrell, A., Quilty, B., & Diamond, D. (2007).  
516 Development of a smart packaging for the monitoring of fish spoilage. *Food Chemistry*, 102(2),  
517 466-470.

518 Pacquit, A., Lau, K. T., McLaughlin, H., Frisby, J., Quilty, B., & Diamond, D. (2006). Development of a  
519 volatile amine sensor for the monitoring of fish spoilage. *Talanta*, 69(2), 515-520.

520 Pourreza, N., & Golmohammadi, H. (2015). Application of curcumin nanoparticles in a lab-on-paper  
521 device as a simple and green pH probe. *Talanta*, 131, 136-141.

522 Priyadarsini, K. I. (2014). The chemistry of curcumin: from extraction to therapeutic agent. *Molecules*,  
523 19(12), 20091-20112.

524 Qin, Y., Liu, Y., Zhang, X., & Liu, J. (2020). Development of active and intelligent packaging by  
525 incorporating betalains from red pitaya (*Hylocereus polyrhizus*) peel into starch/polyvinyl  
526 alcohol films. *Food Hydrocolloids*, 100, 105410.

527 Saliu, F., & Della Pergola, R. (2018). Carbon dioxide colorimetric indicators for food packaging  
528 application: applicability of anthocyanin and poly-lysine mixtures. *Sensors and Actuators B:  
529 Chemical*, 258, 1117-1124.

530 Tønnesen, H. H., Karlsen, J., & van Henegouwen, G. B. (1986). Studies on curcumin and curcuminoids  
531 VIII. Photochemical stability of curcumin. *Zeitschrift für Lebensmittel-Untersuchung und  
532 Forschung*, 183(2), 116-122.

533 Wang, Y. C., Lu, L., & Gunasekaran, S. (2017). Biopolymer/gold nanoparticles composite plasmonic  
534 thermal history indicator to monitor quality and safety of perishable bioproducts. *Biosensors  
535 and Bioelectronics*, 92, 109-116.

536 Wells, N., Yusufu, D., & Mills, A. (2019). Colourimetric plastic film indicator for the detection of the  
537 volatile basic nitrogen compounds associated with fish spoilage. *Talanta*, 194, 830-836.

538 Xiang, H., Sun-Waterhouse, D., Cui, C., Wang, W., & Dong, K. (2018). Modification of soy protein  
539 isolate by glutaminase for nanocomplexation with curcumin. *Food Chemistry*, 268, 504-512.

540 Zhai, X., Li, Z., Shi, J., Huang, X., Sun, Z., Zhang, D., Zou, X., Sun, Y., Zhang, J., Holmes, M., Gong,  
541 Y., Povey, M., & Wang, S. (2019). A colorimetric hydrogen sulfide sensor based on gellan gum-  
542 silver nanoparticles bionanocomposite for monitoring of meat spoilage in intelligent packaging.  
543 *Food Chemistry*, 290, 135-143.

544 Zhai, X., Li, Z., Zhang, J., Shi, J., Zou, X., Huang, X., Zhang, D., Sun, Y., Yang, Z., Holmes, M., Gong,  
545 Y., & Povey, M. (2018). Natural biomaterial-based edible and pH-sensitive films combined with  
546 electrochemical writing for intelligent food packaging. *Journal of Agricultural and Food  
547 Chemistry*, 66(48), 12836-12846.

548 Zhai, X., Shi, J., Zou, X., Wang, S., Jiang, C., Zhang, J., Huang, X., Zhang, W., & Holmes, M. (2017).  
549 Novel colorimetric films based on starch/polyvinyl alcohol incorporated with roselle  
550 anthocyanins for fish freshness monitoring. *Food Hydrocolloids*, 69, 308-317.

551 Zhai, X., Zou, X., Shi, J., Huang, X., Sun, Z., Li, Z., Sun, Y., Li, Y., Wang, X., Holmes, M., Gong, Y.,  
552 Povey, M., & Xiao, J. (2020). Amine-responsive bilayer films with improved illumination  
553 stability and electrochemical writing property for visual monitoring of meat spoilage. *Sensors  
554 and Actuators B: Chemical*, 302, 127130-127141.

555 Zhang, C., Yin, A.-X., Jiang, R., Rong, J., Dong, L., Zhao, T., Sun, L.-D., Wang, J., Chen, X., & Yan, C.-  
556 H. (2013). Time-temperature indicator for perishable products based on kinetically  
557 programmable Ag overgrowth on Au nanorods. *ACS Nano*, 7(5), 4561-4568.

558 Zhang, J., Zou, X., Zhai, X., Huang, X., Jiang, C., & Holmes, M. (2019). Preparation of an intelligent  
559 pH film based on biodegradable polymers and roselle anthocyanins for monitoring pork  
560 freshness. *Food Chemistry*, 272, 306-312.

561 Zhang, X., Lu, S., & Chen, X. (2014). A visual pH sensing film using natural dyes from *Bauhinia*  
562 *blakeana* Dunn. *Sensors and Actuators B: Chemical*, 198, 268-273.

563 Zhu, R., Desroches, M., Yoon, B., & Swager, T. M. (2017). Wireless oxygen sensors enabled by Fe(II)-  
564 polymer wrapped carbon nanotubes. *ACS Sensors*, 2(7), 1044-1050.

565 Zia, J., Paul, U. C., Heredia-Guerrero, J. A., Athanassiou, A., & Fragouli, D. (2019). Low-density  
566 polyethylene/curcumin melt extruded composites with enhanced water vapor barrier and  
567 antioxidant properties for active food packaging. *Polymer*, 175, 137-145.

568

569

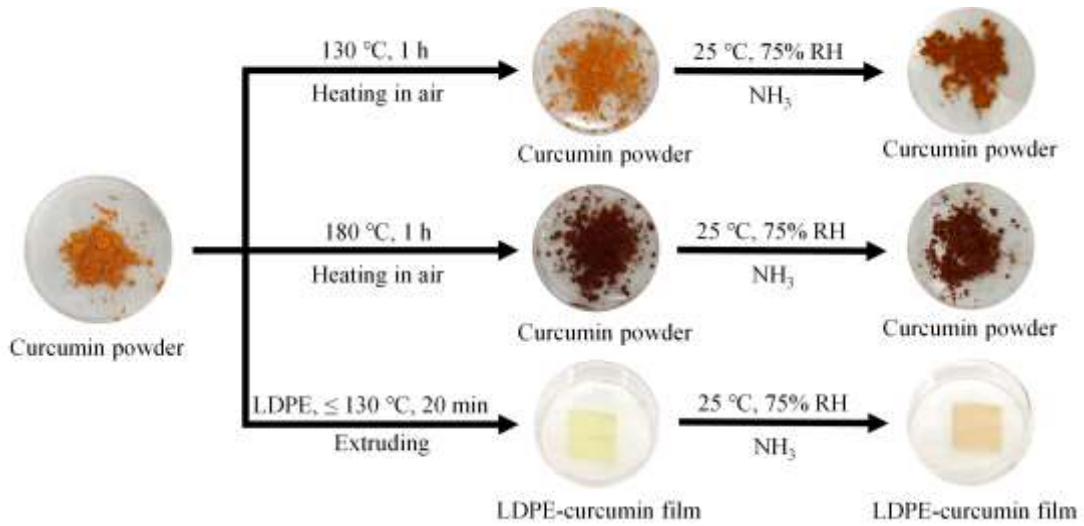


Fig. 1. The photos of curcumin powder and LDPE-curcumin film.

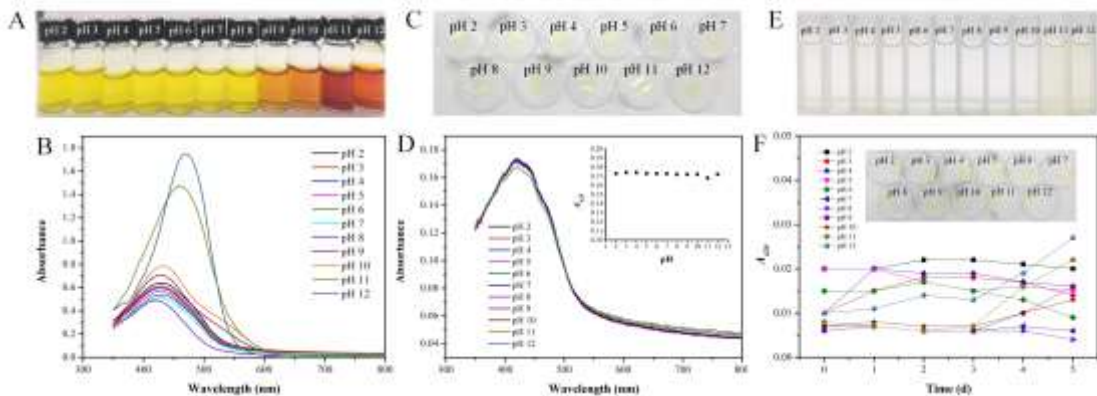
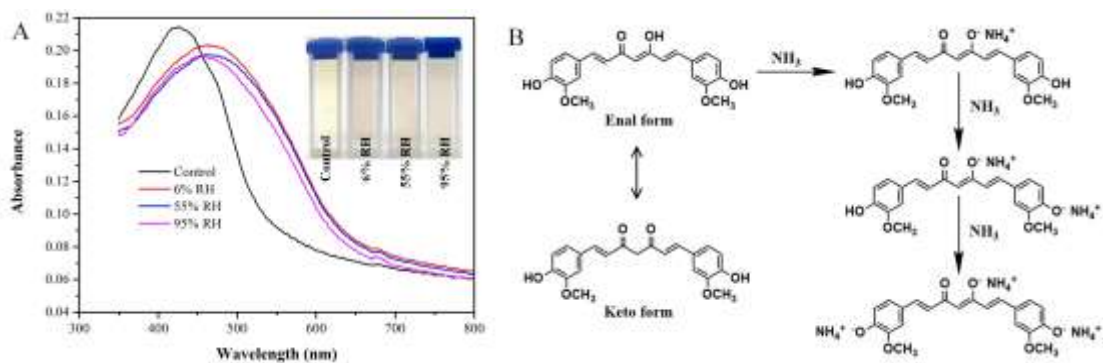


Fig. 2. (A) The photos and (B) UV-Vis spectra of curcumin solution at pH 2-12. (C) The photos and (D) UV-Vis spectra of LDPE-curcumin film immersed in buffer solutions, and inset of (D) is the  $A_{420}$  of the film immersed in buffer solution. (E) The photos and (F)  $A_{420}$  of lixiviums of LDPE-curcumin film immersed in buffer solution, and inset of (F) is the photo of LDPE-curcumin film after immersed in buffer solution for 5 d.

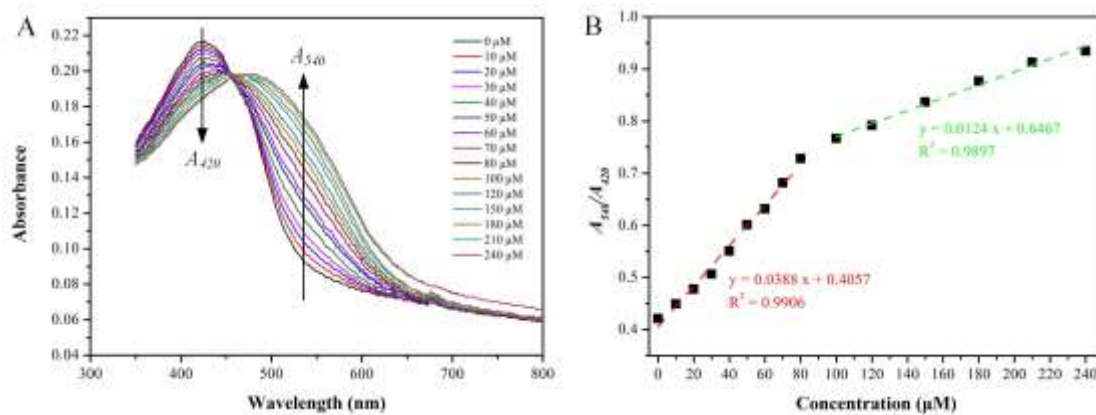


587

588 Fig. 3. (A) UV-Vis spectra and photos (inset) of LDPE-curcumin film after exposed to 200  $\mu\text{M}$  of  
 589  $\text{NH}_3$ , and (B) the proposed reaction mechanism between curcumin and  $\text{NH}_3$

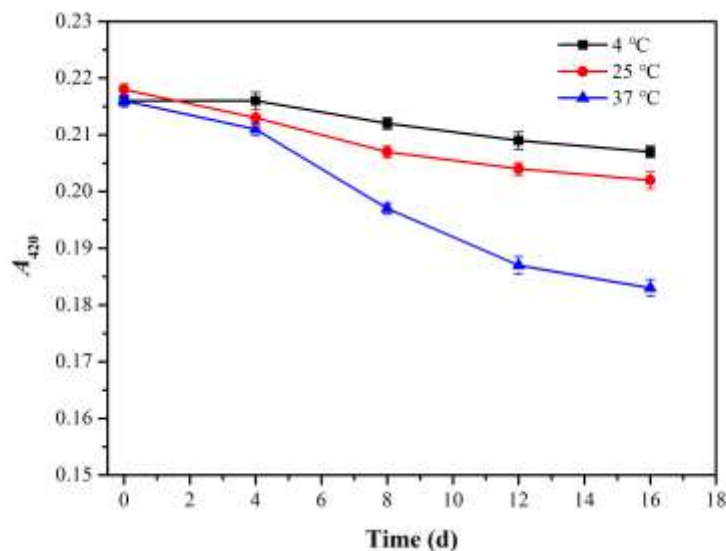
590

591



592

593 Fig. 4. (A) The UV-Vis spectra and (B)  $A_{540}/A_{420}$  of LDPE-curcumin film in response to  $\text{NH}_3$  with  
 594 concentrations of 0-240  $\mu\text{M}$ .

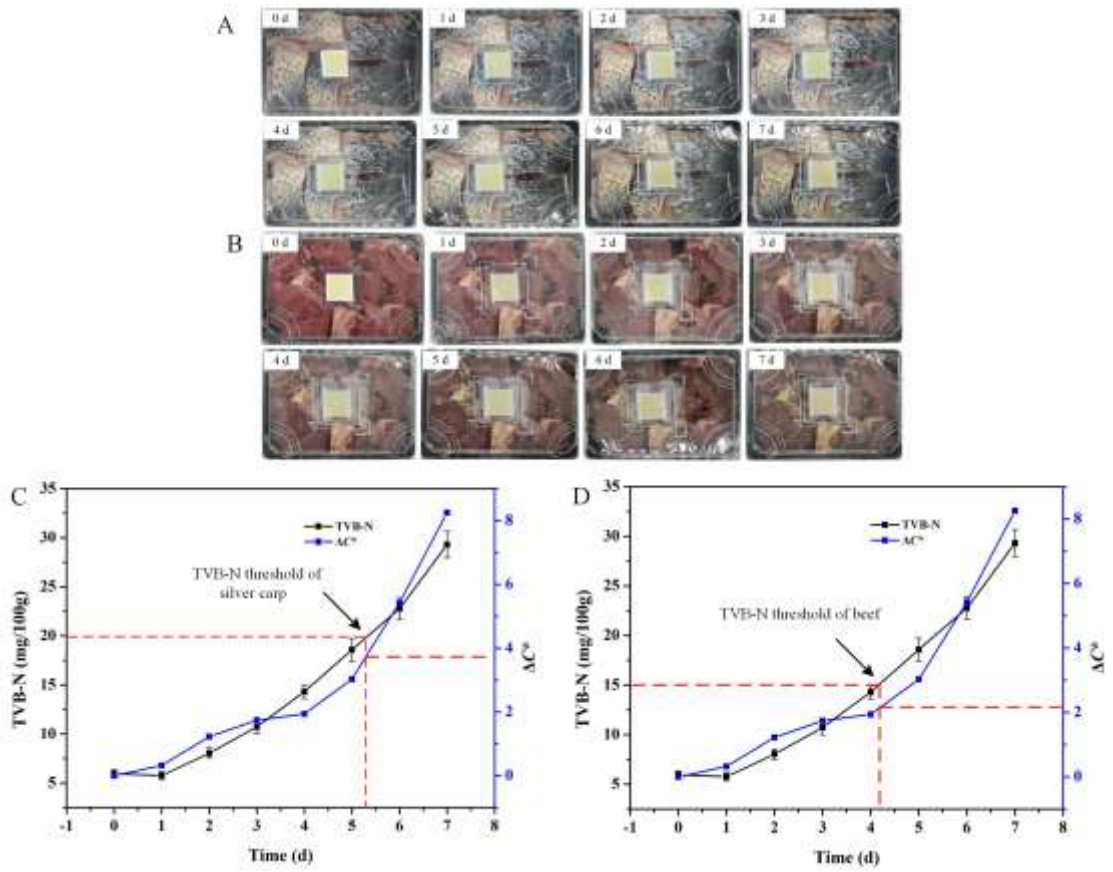


595

596 Fig. 5. The changes of  $A_{420}$  of the LDPE-curcumin film stored at 4, 25 and 37  $^{\circ}\text{C}$ .

597

598



599

600 Fig. 6. The photos of the packages with (A) silver carp and (B) beef, and the relation between TVB-  
 601 N and  $\Delta C^*$  of LDPE-curcumin film for (C) silver carp and (D) beef.

602

603

604

605

606